

Heating-Assisted Atom Transfer in the Scanning Tunneling Microscope

M. Grigorescu¹

Abstract:

The effect of the environmental interactions on the localization probability for a Xe atom trapped in the surface-tip junction of the scanning tunneling microscope is studied in the frame of a stochastic, non-linear Liouville equation for the density operator. It is shown that the irreversible transfer from surface to tip may be explained by thermal decoherence rather than by the driving force acting during the application of a voltage pulse.

PACS numbers: 61.16.Di,73.40.Gk,05.40.+j

Submitted to Z. Phys. B.

http://publish.aps.org/eprint/gateway/eplist/aps1997aug19_001

¹ present address: Institut für Theoretische Physik, Justus-Liebig-Universität Giessen, Heinrich-Buff-Ring 16, D-35392 Giessen, Germany

1. Introduction

Since the first experiments on reversible atom transfer [1], the scanning tunneling microscope (STM) may be considered as the ideal instrument for manipulating atoms or molecules. The bistable operation mode of STM indicate that in a certain geometry the diffusion barrier on surface is high enough to prevent the particle escape from the junction region, and the motion takes place along the outer normal to the surface plane in an asymmetric, one-dimensional, double-well potential (DWP) [2]. However, the mechanism of irreversible atom transfer between the potential wells after the application of a voltage pulse is not yet completely understood.

If the initial center of mass (CM) wave function of the atom is an isomeric state of the static junction potential, then the barrier crossing appears only in special resonance conditions, by quantum coherence oscillations (QCO) [3]. The resonances with long oscillation periods require a very fine tuning of the bias voltage, which cannot be assumed in the present switching experiments. Also, during QCO the tunneling has not an exponential law. Therefore, is a most interesting issue to study the evolution of the atomic CM wave packet dynamics during the voltage pulse, and the decoherence effects produced by the coupling with the environment. This coupling may damp [4] or completely suppress [5] the QCO.

The appropriate frame for the treatment of a quantum dynamics determined both by the unitary evolution in the Hilbert space and by the change in the purity of the states (of the occupation numbers), is provided by the Liouville equation for the density operator. However, this equation can be solved only for very simple systems, and in a physical situation is necessary to find suitable approximations.

The occupation numbers of the energy levels for a Xe atom in the STM junction potential may change in time by the interactions with the electron gas. A partial description of this process is given by the rate equations [2], but for a realistic treatment is necessary to account also the dynamical effects related to the evolution of the non-stationary wave packets, as the QCO.

In this work, the effect of environmental decoherence on the atom dynamics in the STM junction will be described phenomenologically using a modified Liouville equation. This equation is presented in Sec. 2, and is applied to calculate the transition rate induced by the thermal noise. In Sec. 3 are presented numerical results concerning the evolution of the localiza-

tion probability for a Xe atom. At zero temperature, the probability density during a voltage pulse is determined by the evolution of the quantum wave packet in a time-dependent external potential. This evolution is obtained by solving numerically the Schrödinger equation, for symmetric triangular and trapezoidal pulses with -0.8 V at the peak. The environmental decoherence effects are studied using the non-linear Liouville equation for the density operator, at the temperature $T = 4$ K and a constant voltage U . Two values of U are considered, one non-resonant, $U = -0.8$ V, and $U = 1.141$ V, corresponding to the QCO resonance with the highest frequency. The conclusions are summarized in Sec. 4.

2. Brownian quantum dynamics

Let us consider a quantum system with the density operator \mathcal{D} , interacting with a classical heat bath of N_c harmonic oscillators via the bilinear coupling term [6]

$$H_{coup} = x \sum_{i=1}^{N_c} C_i q_i , \quad (1)$$

where x is the coupling operator, C_i are constants and q_i the time-dependent bath coordinates. The evolution of this mixed classical-quantum system can be obtained from the variational equation [7]

$$\delta \int dt \left\{ \sum_{i=1}^{N_c} (\dot{q}_i p_i - h_i) + Tr[\eta^\dagger i\hbar \partial_t \eta - \eta^\dagger (H_0 + H_{coup}) \eta] \right\} = 0 , \quad (2)$$

where $h_i = (p_i^2 + m_i^2 \omega_i^2 q_i^2)/2m_i$ is the classical Hamiltonian for a bath oscillator, H_0 is the Hamiltonian operator for the isolated quantum system, and η, η^\dagger are the "square root operators" defined by the Gauss decomposition of the density operator, $\mathcal{D} = \eta \eta^\dagger$ [8]. In the physical situation of a thermally equilibrated bath with infinite heat capacity, Eq. (2) leads to a Brownian dynamics of the density operator \mathcal{D} , described by the stochastic Liouville equation [7]

$$i\hbar \partial_t \mathcal{D} = [H_0 - x(\xi(t) + f_{\mathcal{D}}(t)), \mathcal{D}] . \quad (3)$$

Here $\xi(t)$ is a random force with zero mean (the noise), while

$$f_{\mathcal{D}}(t) = - \int_0^t dt' \Gamma(t-t') \frac{dTr(\mathcal{D}x)}{dt'} \quad (4)$$

is a friction force with the memory function $\Gamma(t)$. If $\langle\langle * \rangle\rangle$ denotes the average over the statistical bath ensemble at the temperature T , then $\langle\langle \xi(t) \rangle\rangle = 0$, and $\langle\langle \xi(t)\xi(t') \rangle\rangle = k_B T \Gamma(t-t')$, by the fluctuation-dissipation theorem (FDT). The Brownian evolution of \mathcal{D} determined by Eq. (3) preserves the "purity" of the initial state, but decoherence may appear for the average

$$\mathcal{D}_{av}(t) \equiv \langle\langle \mathcal{D} \rangle\rangle(t) = \sum_{r=1}^{N_t} \frac{\mathcal{D}^r(t)}{N_t} \quad (5)$$

calculated over an ensemble of N_t trajectories $\mathcal{D}^r(t)$ generated with the same initial condition, $\mathcal{D}^r(0) = \mathcal{D}_0$. Of particular interest is the case when the initial state of the system is not thermally equilibrated, and $\mathcal{D}_0 = |\psi_0\rangle\langle\psi_0|$, with $|\psi_0\rangle$ a pure state. In this case,

$$\mathcal{D}_{av}(t) = \frac{1}{N_t} \sum_{r=1}^{N_t} |\psi^r(t)\rangle\langle\psi^r(t)| \quad (6)$$

where $|\psi^r(t)\rangle$ is a solution of the modified Schrödinger equation

$$i\hbar\partial_t |\psi^r\rangle = [H_0 - x(\xi(t) + f_D^r(t))] |\psi^r\rangle \quad (7)$$

If the friction may be neglected, then Eq. (3) has the general solution

$$\mathcal{D}^r(t) = e^{-iH_0t/\hbar} \tilde{\mathcal{D}}^r(t) e^{iH_0t/\hbar} \quad (8)$$

with

$$\tilde{\mathcal{D}}^r(t) = \mathcal{T} e^{\frac{i}{\hbar} \int_0^t dt' \xi^r(t') \mathcal{L}_{\tilde{x}(t')}} \rho_0 \quad (9)$$

Here \mathcal{T} denotes the time-ordering operator [9], \mathcal{L}_A is the Lie derivative with respect to the operator A defined by the commutator, $\mathcal{L}_A B \equiv [A, B]$, while

$$\tilde{x}(t) = e^{iH_0t/\hbar} x e^{-iH_0t/\hbar} \quad (10)$$

is the coupling operator in the interaction representation.

The evolution determined by the unitary operator $\exp(-iH_0t/\hbar)$ is the same for all the trajectories appearing in Eq. (5), and therefore the ensemble average may be written as

$$\mathcal{D}_{av}(t) = e^{-iH_0t/\hbar} \tilde{\mathcal{D}}_{av}(t) e^{iH_0t/\hbar} \quad (11)$$

Here $\tilde{\mathcal{D}}_{av}(t)$ denotes the trajectory average of $\tilde{\mathcal{D}}^r(t)$, and can be calculated using the FDT after the expansion of the time-ordered exponential in Eq. (9). Retaining only the first non-vanishing average, the result is

$$\tilde{\mathcal{D}}_{av}(t) = \mathcal{D}_0 - \frac{k_B T}{\hbar^2} \int_0^t dt_1 \int_0^{t_1} dt_2 \Gamma(t_1 - t_2) [\tilde{x}(t_1), [\tilde{x}(t_2), \mathcal{D}_0]] . \quad (12)$$

This formula can be applied to calculate the rate of the noise-induced transitions between the energy eigenstates $\{| E_k \rangle\}$ of H_0 , defined by $H_0 | E_k \rangle = E_k | E_k \rangle$. If initially the system is in the pure state $| E_i \rangle$, then $\mathcal{D}_0 = | E_i \rangle \langle E_i |$, and the rate of the transition $| E_i \rangle \rightarrow | E_f \rangle$ is given by the asymptotic time-derivative

$$\lambda_{fi} = \left. \frac{dv_f}{dt} \right|_{t \rightarrow \infty} \quad (13)$$

of the occupation probability $v_f(t) = \langle E_f | \mathcal{D}_{av}(t) | E_f \rangle = \langle E_f | \tilde{\mathcal{D}}_{av}(t) | E_f \rangle$. Using Eq. (12), this probability is

$$v_f(t) = 2k_B T \frac{|x_{fi}|^2}{\hbar^2} \int_0^t dt_1 \int_0^{t_1} dt_2 \Gamma(t_1 - t_2) \cos \Omega_{fi}(t_1 - t_2) \quad (14)$$

where $x_{fi} = \langle E_f | x | E_i \rangle$ is the matrix element of the coupling operator and $\Omega_{fi} = (E_f - E_i)/\hbar$. In the case of Ohmic dissipation with the static friction coefficient γ , the memory function is proportional to the delta function, $\Gamma(t) = 2\gamma\delta(t)$, and Eq. (13) gives the rate

$$\lambda_{fi} = \frac{2}{\hbar^2} |x_{fi}|^2 \gamma k_B T . \quad (15)$$

This was obtained assuming a classical or quasi-classical behavior of the environmental degrees of freedom. Therefore, it should provide a good approximation when the thermal energy $k_B T$ is greater than the transition energy, $\hbar|\Omega_{fi}|$.

3. Thermally driven atom tunneling

The atom dynamics in the STM junction will be treated assuming that the CM motion is restricted to the X-axis, normal to the surface, and the

potential energy $V(x)$ has an asymmetric, double-well shape. Without external bias, this potential is determined only by the binding interaction energy, and the estimate provided in ref. [2] can be well approximated by the fourth order polynomial

$$V_0(x) = C_0 + C_1x + C_2x^2 + C_3x^3 + C_4x^4 \quad , \quad (16)$$

with $C_0 = 0.45$ meV, $C_1 = 0.77$ meV/Å, $C_2 = -55.64$ meV/Å², $C_3 = -11.59$ meV/Å³, $C_4 = 44.51$ meV/Å⁴. The isomeric minimum of $V_0(x)$ is located at $x_0 = -0.7$ Å, near surface, the barrier top at $x_b = 0$, while the stable minimum at $x_g = 0.89$ Å, near the tip.

At the surface polarization by the voltage U with respect to the tip, the dipole interaction energy changes the potential to $V(x) = V_0(x) - Ed(x)$. Here $E = U/2w$ is the junction electric field, and $d(x)$ is the dipole moment of the Xe atom,

$$d(x) = Q_{eff}x + \mu_0 \left\{ \frac{1}{0.3 + 0.7(w+x)^4/L^4} - \frac{1}{0.3 + 0.7(w-x)^4/L^4} \right\} \quad , \quad (17)$$

where $Q_{eff} \sim 0.1$ e is the average effective charge of Xe [10], $\mu_0 = 0.3$ Debye is the induced dipole moment at the surface, $w = 2.2$ Å, and $L = 1.56$ Å.

If the temperature is zero and there is no dissipation, the atom dynamics during a voltage pulse $U(t)$ can be obtained by integrating the time-dependent Schrödinger equation (TDSE)

$$i\hbar \frac{\partial \psi(x,t)}{\partial t} = \left[-\frac{\hbar^2}{2M} \frac{\partial^2}{\partial x^2} + V_0(x) - \frac{U(t)}{2w} d(x) \right] \psi(x,t) \quad . \quad (18)$$

Assuming that $U(0) = 0$, the initial condition for integration, $\psi(x,0) \equiv \psi_0(x)$, is represented by a Gaussian approximating the isomeric ground state of $V_0(x)$,

$$\psi_0(x) = \left(\frac{c_0}{\pi} \right)^{1/4} e^{-c_0(x-x_0)^2/2} \quad (19)$$

where $c_0 = M\omega_0/\hbar$, M is the Xe mass, and $\omega_0 = \sqrt{M^{-1}d^2V_0/dx^2}|_{x_0}$. The integration of Eq. (18) was performed numerically in a spatial grid $\{x_k\}$, $k = 1, N$, by reduction to a Hamilton system of equations. Thus, if $u_k(t) \equiv \text{Re}(\psi(x_k, t))$ and $v_k(t) \equiv \text{Im}(\psi(x_k, t))$ denote the real, respectively the imaginary part of the wave function $\psi(x, t)$ at the grid point x_k , then Eq. (18) becomes

$$2\hbar \dot{u}_k = \frac{\partial \mathcal{H}}{\partial v_k} \quad 2\hbar \dot{v}_k = -\frac{\partial \mathcal{H}}{\partial u_k} \quad , \quad (20)$$

with

$$\mathcal{H} = \sum_{k=1}^N u_k(Tu)_k + v_k(Tv)_k + V(x_k)(u_k^2 + v_k^2) \quad , \quad (21)$$

$$(Ty)_k = -\frac{\hbar^2}{2Mdx^2} \left[\frac{y_{k+3} + y_{k-3}}{90} - 3\frac{y_{k+2} + y_{k-2}}{20} + 3\frac{y_{k+1} + y_{k-1}}{2} - \frac{49}{18}y_k \right]$$

The Hamiltonian system of Eq. (20) was defined considering $N = 321$ spatial grid points equally spaced by $dx = 0.01 \text{ \AA}$ within the interval $[x_{min}, x_{max}] = [-1.2 \text{ \AA}, 2 \text{ \AA}]$. For a fast integration was used the D02BAF routine of the NAG library [11], with the time step $dt = 6.58 \times 10^{-2} \text{ ps}$. This time step is by two orders of magnitude greater than the time step required for the same accuracy by the leap-frog method.

The solution $\psi(x, t)$ can be used to calculate the time-evolution of the localization probability in the stable well of $V_0(x)$, defined by

$$\rho(t) = \int_0^{x_{max}} |\psi(x, t)|^2 dx \quad . \quad (22)$$

The results obtained when $Q_{eff} = 0$ for a triangular voltage pulse of 20 ns are presented in Fig.1(A), and for a trapezoidal pulse of 7 ns, in Fig.1(C). The bias voltage during the pulse is represented in Fig.1(B) and (D), respectively. The localization probability on the tip presented in Fig.1(A) and 1(C), increases during the pulse front by sudden jumps at certain time moments t_k^A and t_k^C . These time sequences are different, but the sequences U_k^A, U_k^C of the corresponding bias voltages, defined by $U_k^A = U(t_k^A)$ and $U_k^C = U(t_k^C)$ with $U(t)$ of Fig.1(B) and (D) are practically the same (e.g. $-0.08 \text{ V}, -0.164 \text{ V}, -0.24 \text{ V}, -0.32 \text{ V}, -0.4 \text{ V}, -0.48 \text{ V}, \dots$), equally spaced by $\sim 0.08 \text{ V}$. These jump voltages are also very close to the values of U known to ensure a resonant tunneling of the Xe atom between the potential wells by QCO [3]. Therefore, the jumps are explained by the crossing of the resonances during the pulse front, here with arbitrarily chosen slope.

The features noticed above are present also when $Q_{eff} = 0.08 e$, as indicated by the results obtained with a trapezoidal pulse of 7 ns (Fig.2). The increase of ρ during the pulse front keeps the discontinuous character, but the jumps appear at different bias voltages, (e.g. $-0.35 \text{ V}, -0.39 \text{ V}, -0.43 \text{ V}, -0.47 \text{ V}, \dots$), equally spaced by $\sim 0.04 \text{ V}$. This result suggests that the effective charge represents an additional parameter which may shift the values and the spacing of the resonant voltages. In Fig.2(A), ρ becomes 1

during the voltage peak, but the residual value after pulse is small. The propagation in time up to 20 ns of the non-stationary wave packet created by the pulse do not indicate further significant changes in the evolution of ρ .

The extension of the upper time limit of the numerical integration to μs or ms is not yet possible due to the large amount of computer time required. Though, the present results suggest that after the moment when the pulse vanishes, the residual probability of localization on the tip is small.

This behavior was obtained neglecting the dynamical effects produced by the coupling between the atom and the surrounding electron gas. The average features of the atom-electron interaction are reflected by the jump in the junction conductivity at the atom switching, and the potential energy term containing the effective charge, assumed above to be fixed. Though, the experiments on electromigration in metals show that the effective charge is an average quantity which depends on temperature [12]. Therefore, it may have thermal fluctuations, and for a small value as $Q_{eff} \sim 0.1 e$, such effects could be important.

In the following, the fluctuating part of Q_{eff} will be treated phenomenologically, assuming that it can be simulated by an additional dipole interaction in the Hamiltonian, having a structure close to H_{coup} of Eq. (1).

If the Xe atom adsorbed on the surface is thermally equilibrated, and the barrier crossing proceeds by quantum tunneling, then for short times compared to the recurrence time τ_R it could be possible to define the average transfer rate [10]

$$\lambda = \frac{\sum_i e^{-E_i/k_B T^*} \lambda_i}{\sum_i e^{-E_i/k_B T^*}} , \quad (23)$$

where T^* is the effective temperature, E_i are the energies of the isomeric levels and λ_i the corresponding tunneling rates. However, if the system is not equilibrated, and at $t = 0$ the CM wave function is a pure state ψ_0 , then the transfer rate should be defined by

$$\lambda(t) = \frac{\dot{\rho}_{av}(t)}{1 - \rho_{av}(t)} \quad (24)$$

where $\rho_{av}(t) \equiv \langle\langle \rho \rangle\rangle (t)$ is the the average localization probability across the barrier ($x > x_b$), in the stable well of $V(x)$,

$$\rho_{av}(t) = \int_{x_b}^{x_{max}} \langle x | \mathcal{D}_{av}(t) | x \rangle dx . \quad (25)$$

According to Eq. (6), the matrix element $\langle x | \mathcal{D}_{av}(t) | x \rangle$ is given by

$$\langle x | \mathcal{D}_{av}(t) | x \rangle = \frac{1}{N_t} \sum_{r=1}^{N_t} |\langle x | \psi^r(t) \rangle|^2 . \quad (26)$$

The probability amplitude $\langle x | \psi^r(t) \rangle \equiv \psi^r(x, t)$ required here can be obtained by integrating the equation

$$i\hbar\partial_t\psi^r(x, t) = [H_0 - x(\xi^r(t) - \gamma\frac{d\langle x \rangle_r}{dt})]\psi^r(x, t) , \quad (27)$$

where $\langle x \rangle_r \equiv \langle \psi^r | x | \psi^r \rangle$ and

$$H_0 = -\frac{\hbar^2}{2M}\frac{\partial^2}{\partial x^2} + V_0(x) - \frac{U}{2w}d(x) . \quad (28)$$

The average in Eq. (26) was calculated using $N_t = 100$ solutions $\psi^r(t)$ of Eq. (27) at the environmental temperature $T = 4$ K and U constant. Each solution was obtained considering $\xi^r(t)$ at the moment $t_n = ndt$ of the form $\xi^r(t_n) = R_n\sqrt{2k_B T\gamma/dt}$ where $\{R_n, n = 1, 2, 3, \dots\}$ is a sequence of Gaussian random numbers with 0 mean and variance 1. This choice ensures the discrete form of the FDT, $\langle\langle \xi(t_j)\xi(t_k) \rangle\rangle = 2k_B T\gamma\delta_{t_j t_k}/dt$.

The static effective charge parameter in $d(x)$ is chosen $Q_{eff} = 0$ and the friction coefficient is $\gamma = 0.1 \hbar/\text{\AA}^2$. This corresponds to a partial damping rate $\gamma/M \sim 5$ GHz, small compared to the total estimated rate of vibrational relaxation, ~ 30 GHz [15].

At $t = 0$ the atom is supposed to be in a pure state localized near the surface, and the initial condition for integration is the ground state ψ_0 of the modified potential

$$V_{mod}(x) = \begin{cases} V_0(x) - \frac{U}{2w}d(x) & \text{if } x \leq x_b \\ V_0(x_b) - \frac{U}{2w}d(x_b) + \alpha(x - x_b)^2 & \text{if } x > x_b \end{cases} ,$$

obtained by replacing the stable well of $V(x)$ by a harmonic term. When U decreases near the point when the barrier disappear, this procedure provides a better approximation for the isomeric ground state of $V(x)$ than the Gaussian wave packet of Eq. (19).

The state $\psi_0(x)$ was obtained numerically by the Runge-Kutta integration of the stationary Schrödinger equation

$$\left[-\frac{\hbar^2}{2M}\frac{d^2}{dx^2} + V_{mod}(x)\right]\psi_0(x) = E_0\psi_0(x) \quad , \quad (29)$$

where V_{mod} is defined using $\alpha = 0.1$.

The average localization probability on the tip $\langle\langle \rho \rangle\rangle$ and the average energy $\langle\langle H_0 \rangle\rangle \equiv Tr[H_0 \langle\langle \rho \rangle\rangle]$ when $U = -0.8$ V are represented in Fig. 3(A) and (B) by solid lines. The time-dependence of $\langle\langle \rho \rangle\rangle$ can be well approximated in this case by the exponential law

$$\rho_f(t) = 1 - e^{-\lambda_1 t} \quad . \quad (30)$$

The rate constant extracted by fit is $\lambda_1 = 210$ MHz, two orders of magnitude above the WKB tunneling rate, $\lambda_{WKB} = 6.2$ MHz. The WKB rate characterizes the non-dissipative tunneling for times smaller than the recurrence time, $\tau_R \sim 2$ ps. For longer times, the integration of Eq. (27) with $\xi = 0$, $\gamma = 0$, shows that $\rho(t)$ has the anharmonic oscillatory evolution pictured in Fig.3(A) by dashed line. These oscillations contain high and low frequency components, indicating that the initial wave packet is a superposition of several eigenstates of H_0 . During the low frequency oscillation the maximum attained by ρ is $\rho_m \sim 0.5 \cdot 10^{-3}$, while the oscillation amplitude of the average position, $\langle x \rangle$, is $A_x = (\langle x \rangle_{max} - \langle x \rangle_{min})/2 \sim 10^{-3}$ Å.

The low frequency oscillation may be understood assuming that the main components of ψ_0 are two eigenstates ψ_i and ψ_f of H_0 close in energy, but localized in the isomeric, respectively in the stable well of $V(x)$. In this case, the matrix element $|x_{fi}|$ is well approximated by $A_x/\sqrt{\rho_m} = 0.045$ Å. With this value and γ , T used to calculate $\langle\langle \rho \rangle\rangle$, Eq. (15) gives an inelastic tunneling rate $\lambda_{fi} = 209$ MHz, very close to λ_1 extracted by fit.

The two-state approximation becomes particularly suited when the potential is tuned on a QCO resonance [13]. At resonance ψ_0 is a linear superposition of two quasi-degenerate eigenstates of the Hamiltonian, ψ_d , ψ_u each being localized with probability 1/2 in either well. Their energies $E_d \approx E_u$ are such that the average level spacing $2\pi\hbar/\tau_R$ is much greater than $\Delta = |E_u - E_d|$, and the localization probability of ψ_0 "across the barrier" is

$$\rho_{QCO}(t) = \frac{1}{2}\left(1 - \cos\frac{2\pi t}{T}\right) \quad , \quad (31)$$

oscillating with the period $T = 2\pi\hbar/\Delta$, greater than τ_R .

The QCO's of the STM Hamiltonian have an important role in the increase of the atom transfer probability during the pulse front, but they are also very sensitive to the environmental decoherence [14]. To study the environmental effects on the atomic QCO the bias voltage was fixed at the resonant value $U_r = -1.141$ V when Xe oscillates with the shortest period, $T = 28.74$ ps. Without environment coupling, ($\gamma = 0$), the localization probability near the tip for the initial wave packet ψ_0 obtained from Eq. (29) is pictured in Fig.4(A) by dashed line. During this oscillation $\rho_m \approx 1$, $A_x \approx 0.48$ Å, and despite the anharmonicities, $\rho(t)$ is relatively close to $\rho_{QCO}(t)$. At the energy of ψ_0 the WKB tunneling rate is ~ 50 GHz and $\tau_R \sim 3$ ps.

For an environmental temperature of $T = 4$ K, the thermal energy is $k_B T = 0.34$ meV, greater than the doublet splitting, $\Delta = 0.14$ meV, and the decoherence effects should be important. The statistical average $\langle\langle \rho \rangle\rangle$ defined by Eq. (25) was calculated using $N_t = 100$ solutions of Eq. (27), and the result is pictured in Fig.4(A) by solid line. The corresponding average of the energy, $Tr[H_0 \langle\langle \rho \rangle\rangle]$ is shown in Fig.4(B).

The average localization probability of Fig.4(A) has damped oscillations which can be well approximated by the formula

$$\rho_f(t) = 1 - ue^{-\lambda_1 t} - (1 - u)e^{-\lambda_2 t} \cos\left(\frac{2\pi t}{T + \delta}\right) . \quad (32)$$

The parameters obtained by fit are $\lambda_1 = 3.6$ GHz, $\lambda_2 = 33$ GHz, $\delta = 1.6$ ps and $u = 0.495$.

In a two-state system (ψ_u, ψ_d) coupled to the environment the QCO amplitude is damped with the rate λ_{ud} of the intradoublet transitions $\psi_u \leftrightarrow \psi_d$ [4], and asymptotically the system arrives in the mixed state of maximum entropy [7]. In the present case ψ_0 is not a superposition of two states only, but Eq. (15) with the matrix element $|x_{ud}| \approx A_x = 0.48$ Å gives $\lambda_{ud} = 24$ GHz, close to λ_2 obtained by fit.

4. Summary and conclusions

The atom transfer in the scanning tunneling microscope is a complex non-stationary phenomenon, reflecting a dynamical interplay between unitary evolution in Hilbert space and the environmental decoherence.

A phenomenological description of a quantum system interacting bilinearly with a classical heat bath of harmonic oscillators is provided by the modified Liouville equation presented in Sec. 1. This equation may be derived from a variational principle (Eq. (2)), and has a Langevin form, containing stochastic and frictional terms.

The effects of a voltage pulse on the localization probability ρ for a Xe atom prepared initially in a pure state localized on the STM surface was investigated by numerically integrating the TDSE (Eq.(18)). In these calculations the environmental interactions are neglected, and the voltage pulse is assumed of symmetric triangular and trapezoidal shape. The results indicate a stepwise increase of ρ at the moments when the pulse front is near a resonant bias voltage for the isomeric ground state. The resonant values depend on the effective charge, being equally spaced by ~ 0.08 V when $Q_{eff} = 0$, and by ~ 0.04 V when $Q_{eff} = 0.08$ e. However, the evolution of the non-stationary state created by the pulse do not indicate an asymptotic behavior characteristic to exponential decay.

The atom dynamics at finite temperature was investigated in the frame of the stochastic, non-linear Liouville equation (Eq. (3)). The spectrum of the environmental noise was assumed to be flat (white noise), parameterized by the static friction coefficient γ . This has a value corresponding to weak damping, and the effective temperature was considered the same as the environmental temperature, $T = 4$ K.

The ensemble average of the energy increases during tunneling, (Fig.3(B) and 4(B)), but within the time interval of 100 ps investigated here the atom is not thermalized. The evolution of $\langle\langle \rho \rangle\rangle$ at resonance ($U = -1.141$ V), consists of an incoherent superposition between damped QCO and exponential decay. In the non-resonant case ($U = -0.8$ V) the tunneling law is close to exponential, with a rate proportional to the product γT (Eq. (15)). This result can provide a basis for understanding the current dependence of the atom transfer rate, because the friction coefficient as well as the effective temperature should be functions of the electron tunneling current.

References

- [1] D. M. Eigler, C. P. Lutz, W. E. Rudge, *Nature* **352**, 600 (1991).
- [2] R. E. Walkup, D. M. Newns, Ph. Avouris, *Phys. Rev. B* **48**, 1858 (1993).
- [3] M. Grigorescu, P. Budau, N. Carjan, *Phys. Rev. B* **55**, 7244 (1997).
- [4] V. A. Benderskii, V. I. Goldanskii, D. E. Makarov, *Phys. Rep.* **233**, 195 (1993).
- [5] A. J. Bray, M. A. Moore, *Phys. Rev. Lett.* **49**, 1545 (1982).
- [6] P. Hänggi, P. Talkner, M. Borkovec, *Rev. Mod. Phys.* **62**, 251 (1990).
- [7] M. Grigorescu, quant-ph/9709033
- [8] B. Reznik, *Phys. Rev. Lett.* **76**, 1192 (1996).
- [9] J. D. Bjorken, S. D. Drell, *Relativistic Quantum Fields*, Mc Graw-Hill Book Company, New York, 1965, p. 178.
- [10] J. J. Saenz, N. Garcia, *Phys. Rev. B* **47**, 7537 (1993).
- [11] *The NAG Fortran Library Manual, Mark 15*, 1st Edition, June (1991).
- [12] A. H. Verbruggen, *I. B. M. J. Res. Dev.* **32**, 93 (1988).
- [13] J. A. Leggett, S. Chakravarty, A. T. Dorsey, M. P. A. Fisher, A. Garg, W. Zenger, *Rev. Mod. Phys.* **59**, 1 (1987).
- [14] M. Grigorescu, report IFIN-HH Bucharest FT-416-1996 / APS e-print aps1996dec10_001, *Rom. J. Phys.* **7-8** (1997), in press.
- [15] G. P. Salam, M. Persson, R. E. Palmer, *Phys. Rev. B* **49**, 10 655 (1994).

Figure Captions

Fig. 1. Atom tunneling at $Q_{eff} = 0$ without environment coupling. ρ and U as a function of time for a triangular pulse of 20 ns (A),(B) and a trapezoidal voltage pulse of 7 ns (C),(D).

Fig. 2. Atom tunneling at $Q_{eff} = 0.08 e$ without environment coupling. ρ (A) and U (B) as a function of time for a trapezoidal voltage pulse of 7 ns.

Fig. 3. $\langle\langle \rho \rangle\rangle$ (A, solid) and $\langle\langle H_0 \rangle\rangle$ (B) at $U = -0.8$ V for $T = 4$ K, $\gamma = 0.1\hbar/\text{\AA}^2$, compared to ρ at $\gamma = 0$ (A, dash), as a function of time.

Fig. 4. $\langle\langle \rho \rangle\rangle$ (A, solid) and $\langle\langle H_0 \rangle\rangle$ (B) at $U = -1.141$ V, for $T = 4$ K, $\gamma = 0.1\hbar/\text{\AA}^2$, compared to ρ at $\gamma = 0$ (A, dash), as a function of time.

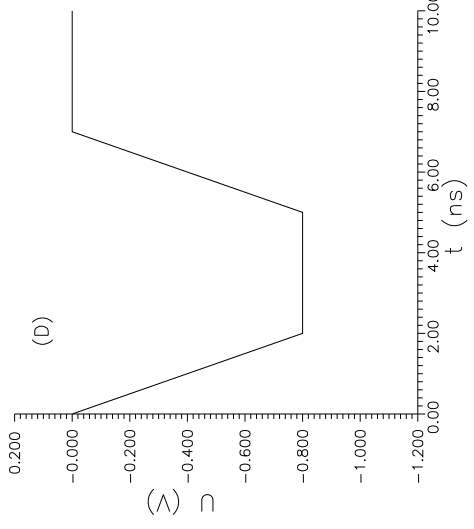
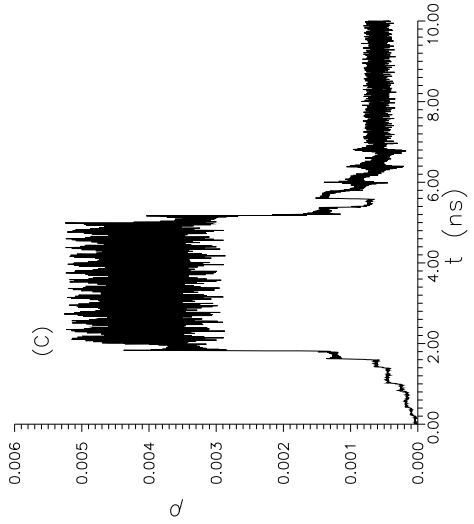
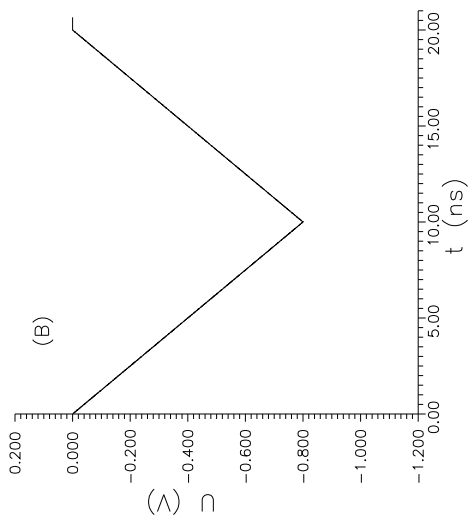
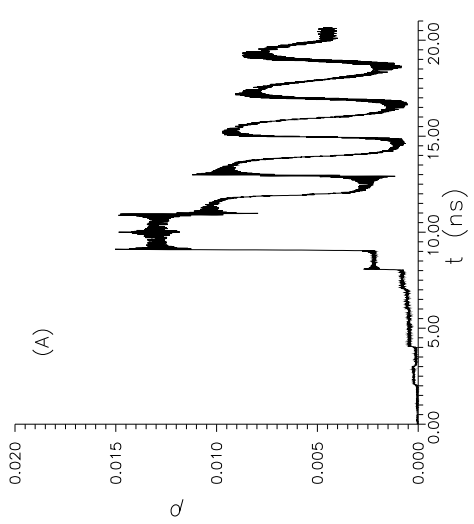


Fig. 1

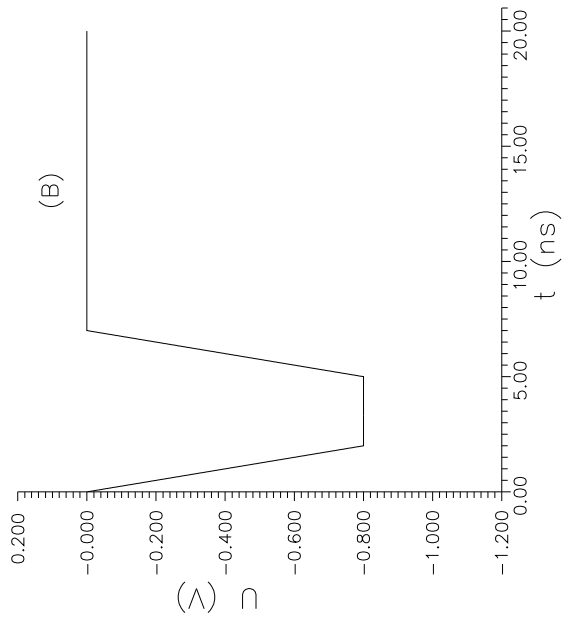
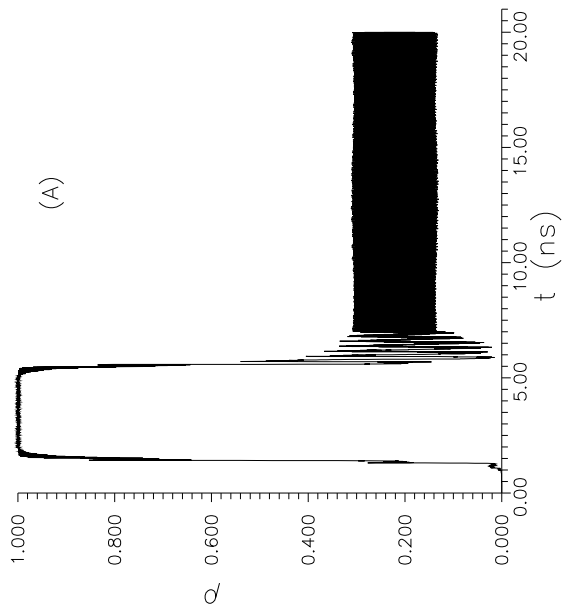


Fig.2

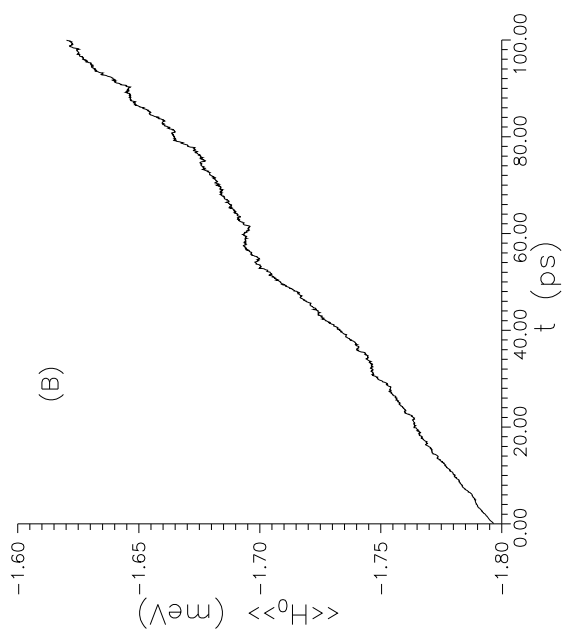
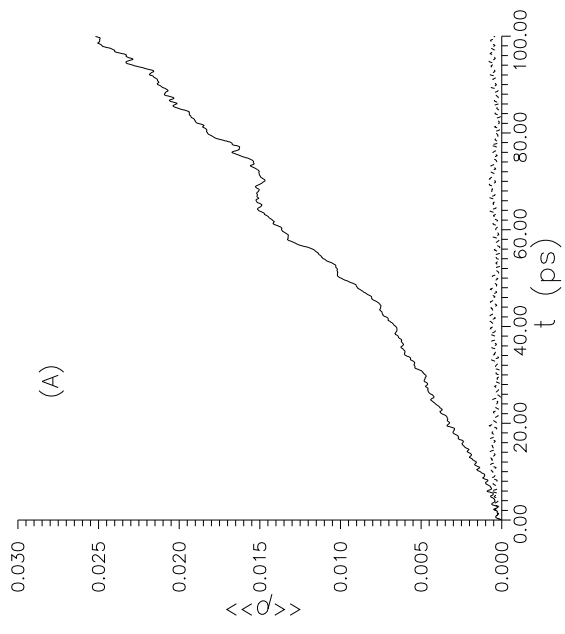


Fig. 3

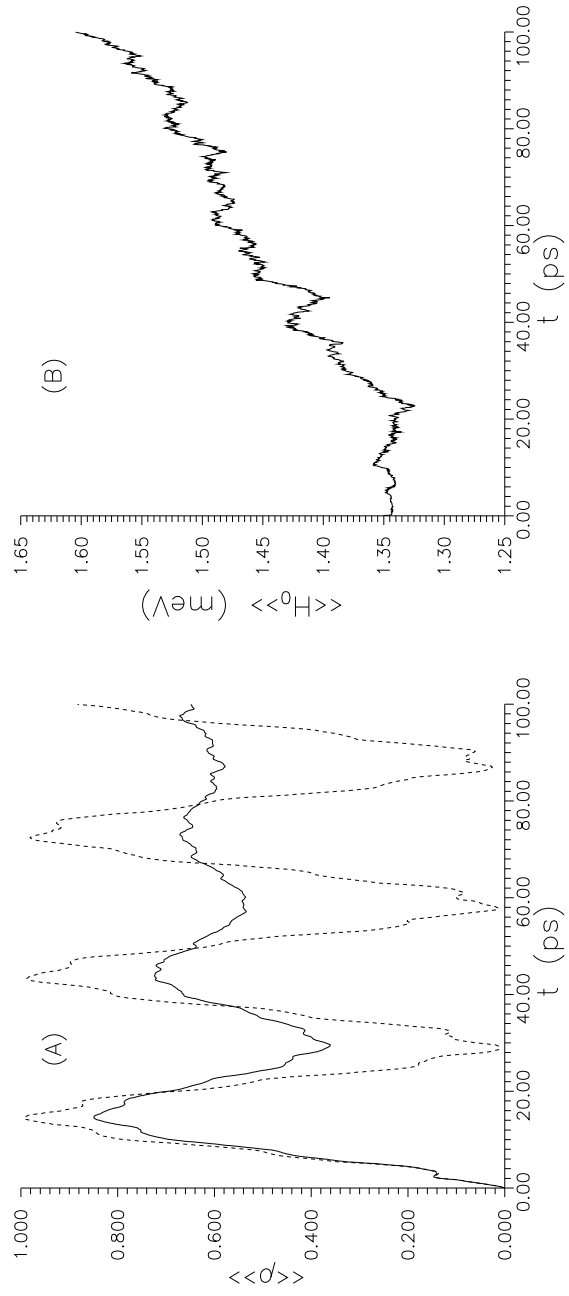


Fig.4